Carbonates Evaporites
DOI 10.1007/s13146-013-0166-1

ORIGINAL ARTICLE

A hydrogeochemical approach for identifying salinization processes in the Cenomanian–Turonian aquifer, south-eastern Tunisia

Narjess Ben Cheikh · Kamel Zouari · Brahim Abidi

Accepted: 3 July 2013

Abstract In southern Tunisia, the Cenomanian–Turonian aquifer constitutes one of the main aquifer systems. It represents an important socioeconomic interest in the region. However, the local increase of groundwater salinity remains the biggest problem to its exploitation, particularly in the northern part. Thus, a combined hydrogeologic and isotopic survey using several chemical and isotopic tracers was conducted to evaluate the principal mineralization process of this aquifer. Stratigraphic and tectonic conditions seem to play an important role in the spatial evolution of groundwater quality in the study area. In fact, the results allow identifying the dissolution of evaporitic rocks as the main cause of groundwater salinization.

Keywords Cenomanian–Turonian aquifer · Groundwater salinity · Chemical and isotopic tracers · Dissolution · Tunisia

Introduction

The study area is located in the south-eastern part of Tunisia and covers a region bordered by Dahar Mountains to the south, the western part of Northern Chotts Range to the west, the Sabkha Noual to the north and reaches eastward as far as the Mediterranean Sea (Fig. 1). It is characterized by an arid to semi-arid climate. The annual precipitation is characterized by its irregularity. In such environments, deep aquifers remain commonly as the only source of water. Indeed, the Miocene and Quaternary aquifers, constituting sands and sandstones, have provided the main part of the water supply since 1940. However, intensive exploitation of these aquifers during the last few years has induced declining water levels and increased risk of groundwater salinization. In such a situation, it seemed indispensable to look for waters in deeper horizons. Indeed, the calcareous dolomitic Cenomanian–Turonian is a confined aquifer under the Senonian limestones and is sometimes in direct contact with the Miocene sands. Exploited for the first time in 1984, this aquifer was especially intended to satisfy the agricultural water demands of the Matmata area to the south. However, in the northern part, it does not show encouraging results due to intense mineralization of its groundwaters. The main objective of this study is to explain the local increase in groundwater salinity of the Cenomanian–Turonian aquifer using geological and geochemical tools.

N. Ben Cheikh (✉) · K. Zouari
Laboratoire de Radio-Analyses et Environnement,
Ecole Nationale d'Ingénieurs de Sfax, BP 1173,
3038 Sfax, Tunisia
e-mail: bencheikh_narjess@yahoo.fr

B. Abidi
Arrondissement des Ressources en Eau de Gabès,
Route de Médenine, 6019 Gabès, Tunisia

Geological and hydrogeological setting

On the geological map (Fig. 1), the sedimentary succession extends from the lower Cretaceous which outcrops along the northern Chotts Range to the Quaternary sediments.

Triassic extrusions, which always outcrop in an abnormal tectonic situation, are identified at diverse points along the Gafsa fault (Ouled Grib Slimane 1994) as in the diapir of Hadifa Mountain (located in the eastern part of the northern Chotts Range), which constitutes on the Tunisian Atlas scale the last outcropping of Triassic deposits to the south (Abbes et al. 1994). These are composed of white

Published online: 02 August 2013

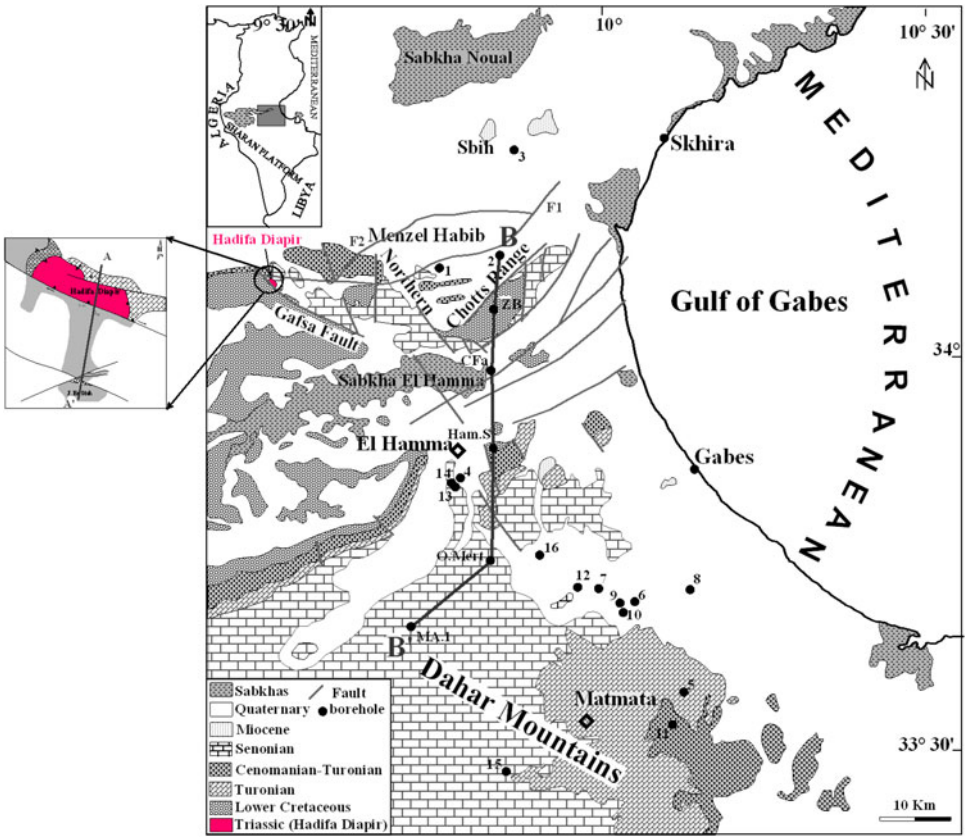

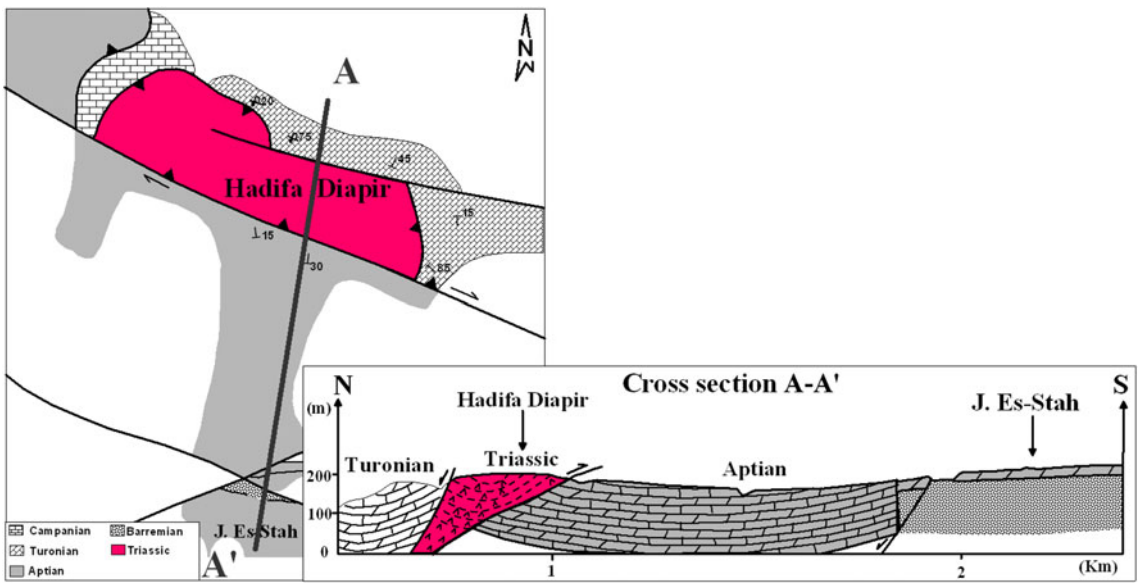

Fig. 1 Simplified geological map of the study area

Fig. 2 Structural cross section (A–A′) of the Hadifa Diapir

dolomite, anhydrite, celestite, bipyramidal quartz, red clays and salt. Dolomite crystals range from a few millimeters to few centimeters in width (Ihsan and Abdallah 2006).

In this region, several studies (Abdallah et al. 2000; Louhaichi and Tlig 1993; Abdeljaouad 1983; Zouaghi et al. 2007) showed the synsedimentary intervention of Triassic formations during the Upper Cretaceous sedimentation. Indeed, the Triassic formations appear to be in direct contact with the neighboring Upper Cretaceous series (Fig. 2).

The continental formations of Lower Cretaceous, which contain the CI (Continental Intercalaire) aquifer, outcrop in

the Zemlet El Beida Mountain (ZB) and constitute the main water-bearing formation in the region of El Hamma.

Turonian formations outcrop in the south and extend to approximately 760 km^2 along the eastern border of Dahar Mountains. It is represented by fissured dolomitic limestones and massive dolomites forming a very remarkable cliff in all the Tunisian South (Busson 1967). Indeed, the significant extension of outcropping Turonian deposits, the

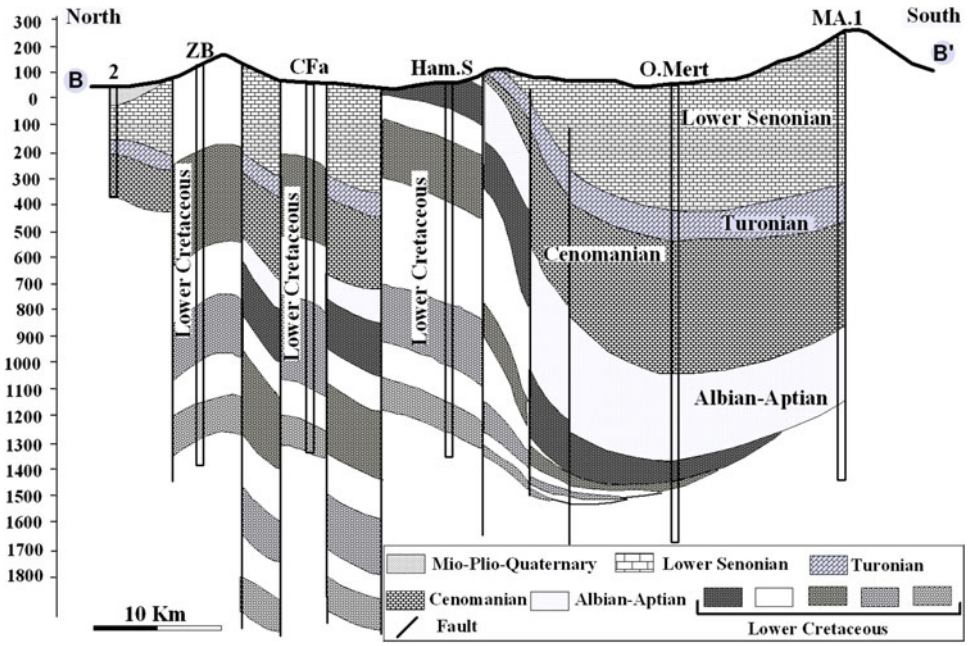

Fig. 3 Hydrogeological cross section (B–B′)

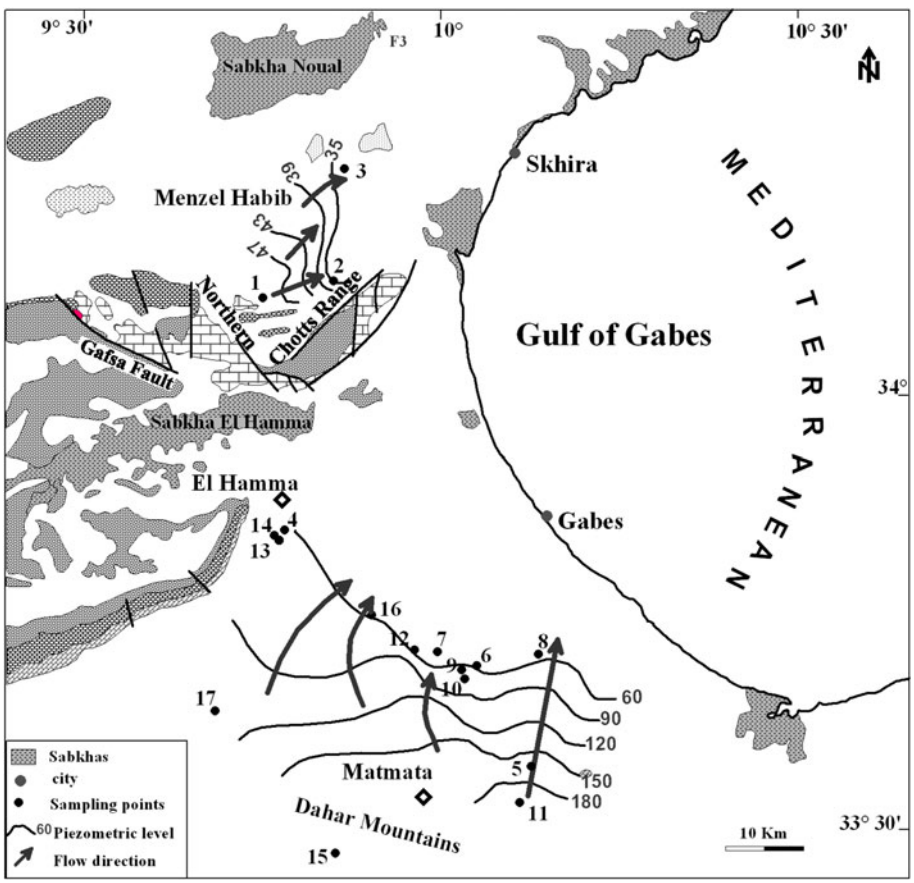

Fig. 4 Location of sampled points (Jannuary 2008) and piezometric contour map of the Cenomanian–Turonian aquifer

limestones permeability as well as the important annual precipitation are all factors which favored the infiltration of an important quantity of waters into the Matmata area.

In depth, the Cenomanian–Turonian deposits are mainly composed of marls, dolomites and fissured limestones and are known as the Zebbag formation (Abdallah et al. 1995; Christian and Hassen 1995). They constitute the principal water-bearing formation in the Matmata area and were met with almost the same lithology in the Menzel Habib and Sbih regions to the north (Fig. 3). These calcareous deposits are characterized by variable thickness up to 300 m and are strongly fissured, with the transmissivity ranging from 2.10^{-4} to 3.10^{-5} m^2/s. The values of specific discharge show also a big variation between 0.4 and 300 l/s/m in relation to the degree of fissuring of limestones.

In Tunisia, the Triassic extrusions align in several tectonic directions (NW–SE) as in the Hadifa Mountain. Overall, the Triassic Diapir occupies three settings: outcrops, buried dome and injected along normal faults (Ihsan and Abdallah 2006).

Geophysical data show that normal faults are oriented appreciably to the east–west in the studied area. This

Table 1 Physical and chemical parameters of the analyzed groundwater samples

Well	Aquifer	Depth (m)	pH	EC (µS/cm)	T (°C)	TDS (mg/l)	Na^+ (mg/l)	Cl^- (mg/l)	SO_4^{2-} (mg/l)	K^+ (mg/l)
1	C–T	150–180	7.4	21,610	20.7	18,600	4,853	7,881	2,760	144
2	C–T	365–402	7.5	26,400	24.2	20,910	5,175	8,662	3,000	159
3	C–T	235–277	7.2	21,200	21	18,930	4,499	6,390	3,146	200
4	C–T	–	7.86	4,490	29.5	3,150	496	923	1,296	42
5	C–T	45–80	7.18	3,450	23.7	2,840	289	710	1,180	10
6	C–T	148–169	7.48	4,690	20.2	3,800	427	639	1,788	17
7	C–T	410–571	7.55	3,740	25	3,250	368	497	1,228	18
8	C–T	233–354	7.23	3,480	23.3	2,900	358	497	1,161	13
9	C–T	188–220	7.56	4,390	–	3,400	510	639	1,560	17
10	C–T	148–169	7.8	4,220	–	3,800	487	568	1,608	14
11	C–T	50–67	7.18	3,400	23.7	2,920	289	994	1,142	12
12	C–T	515–544	7.66	3,850	24.8	2,750	455	710	1,440	23
13	C–T	516–600	7.85	4,280	29	3,200	496	923	1,200	41
14	C–T	362–462	7.53	3,620	–	2,680	473	781	1,104	34
15	C–T	–	7.75	1,680	27	1,200	240	271	684	–
16	C–T	–	7.54	4,060	–	2,720	322	497	1,152	–

Well	Ca^{2+} (mg/l)	Mg^{2+} (mg/l)	HCO^{3-} (mg/l)	CO_3^{2-}(mg/l)	IS Gyp	IS Hal	IS An	V-SMOW		^{14}C (pmc)
								δ^2H (‰)	$\delta^{18}O$ (‰)	
1	1,088	412	48	0	−0.01	−3.22	−0.23	−47.8	−6.68	–
2	1,392	268	164	0	0.11	−3.15	−0.10	−46.5	−6.86	38
3	960	187	292	0	0.03	−3.34	−0.18	−45.5	−6.31	12.6
4	336	134	134	0	−0.38	−5.03	0.6	−58.6	−8.31	–
5	384	115	286	0	−0.34	−5.37	−0.56	−32.5	−6.05	43
6	352	182	158	0	−0.27	−5.26	−0.49	−49.7	−6.92	11.4
7	320	144	152	0	−0.39	−5.42	−0.61	−51.6	−7.01	9.5
8	256	163	146	0	−0.50	−5.43	−0.72	−49.3	−6.97	12.5
9	352	153	176	0	−0.31	−5.18	−0.53	–	–	–
10	352	172	134	0	−0.30	−5.25	−0.52	–	–	–
11	336	139	237	0	−0.41	−5.23	−0.63	–	–	–
12	272	201	158	0	−0.44	−5.18	−0.66	–	–	–
13	288	153	140	0	−0.47	−5.03	0.69	−57.8	−8.31	–
14	320	152	152	0	−0.45	−5.12	0.67	–	–	–
15	222	66	164	0	−0.64	−5.83	0.86	–	–	25.7
16	360	72	163	0	−0.34	−5.47	0.56	−52.23	–	11

C–T Cenomanian–Turonian, *Depth* depth of the water-bearing formation (m), *EC* electrical conductivity (µS/cm), *TDS* total dissolved salts (mg/l), *IS* saturation indices, *Gyp* gypsum, *Hal* halite, *An* anhydrite

induces a distinct lateral compartmentalization. Indeed, the F1 fault, which originates in the Hadifa Diapir in the west, extends eastward and passes quite near the C-T1 and C-T2 boreholes to the east (Fig. 1).

The piezometric map of the Cenomanian–Turonian aquifer shows a general SW–NE flow from bordering mountains (northern Chotts Range and Dahar Mountains) toward the Mediterranean Sea in relation to the structural and especially topographic conditions (Fig. 4). In spite of the limited number of existing boreholes in the Menzel Habib-Sbih area, the hydraulic head still reveals an SW–NE flow in the direction of the coastal plain.

Sampling and analyses

Groundwater samples were collected from existing boreholes in January 2008 (Fig. 4) and chemically analyzed for ^{18}O, ^{2}H and ^{14}C. The non-conservative chemical and physical parameters (temperature, pH, electrical conductivity) were measured in the field. Major elements (Cl^-, SO_4^{2-}, Ca^{2+}, Mg^{2+}, Na^+, K^+ and HCO_3^-) were analyzed by ion liquid chromatography at the Laboratory of Radio-Analysis and Environment of the National School of Engineers of Sfax (Tunisia). Stable isotope compositions (^{18}O, ^{2}H) of the groundwater samples were determined by isotope ratio mass spectrometry in the Isotope Hydrology Laboratory of the International Atomic Energy Agency (IAEA) in Vienna and are reported in conventional notation in δ per mil with regard to the international standard V-SMOW. Typical precisions are $\pm$ 0.1 and $\pm$ 1.0 ‰ for oxygen and deuterium, respectively. Radiocarbon analyses were also completed at the Laboratory of Radio-Analysis and Environment of the National School of Engineers of Sfax by using benzene synthesis and liquid scintillation spectrometry (Fontes 1971). The measured ^{14}C concentrations are expressed as percent of modern carbon (pmc) with an analytical uncertainty of 0.3 pmc.

Results and discussion

Geochemical study

The physical and chemical parameters of Cenomanian–Turonian groundwater are represented in Table 1. The

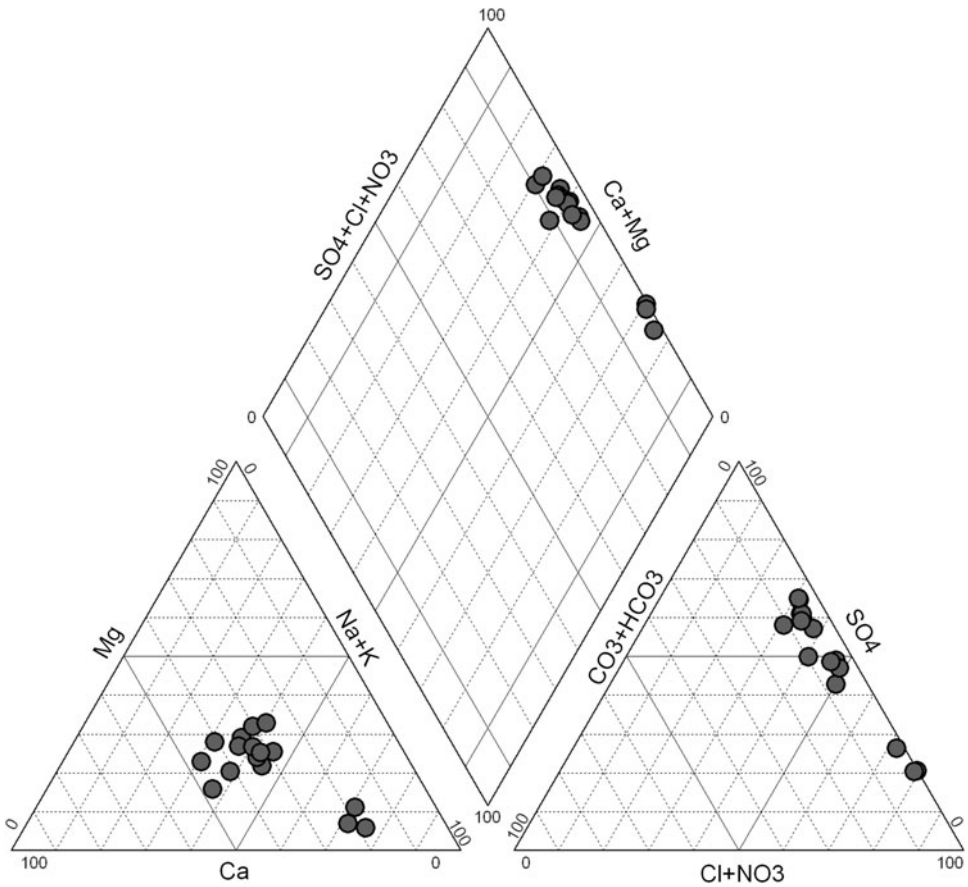

Fig. 5 Piper diagram of the Cenomanian–Turonian groundwater samples

groundwater temperature varies from 20.2 to 29.5 °C independently of the water-bearing formation depth. The highest values, probably due to the influx of groundwater of the CI (Continental Intercalaire) aquifer through existing faults (Abidi 2001), were obtained in the El Hamma region (samples 4 and 13). The electrical conductivity (EC) ranged from 1,680 to 26,400 µs cm^{-1}. These high CE measurements were well correlated to high total mineralization which varied largely between 1,200 and 20,910 mg l^{-1}. The lowest TDS values were obtained in the Matmata region where the spatial distribution of TDS was somewhat similar. However, in the Menzel Habib-Sbih area, the salinity of groundwater (samples: 1, 2, 3) increased and exceeded 20,000 mg l^{-1}.

The major ion composition of water analyses is depicted in the Piper trilinear equivalence diagram (Fig. 5). It appears that Cenomanian–Turonian groundwater has been classified into two major water types: (1) In the Matmata region, major cations reveal similar concentrations intermediate between Na^+ and Ca^{2+} content. In terms of anions, the groundwater is typically enriched in SO_4^{2-}. (2) In the Menzel Habib-Sbih area, groundwater seems to be rather rich in Na^+ and Cl^-. This trend reflects the complexity of hydro-geochemical processes that control groundwater salinity. Indeed, the unexpected high salinities, only felt at local scale in the northern part of the study area, can be related to the outcropping Triassic in the Hadifa Diapir to the west.

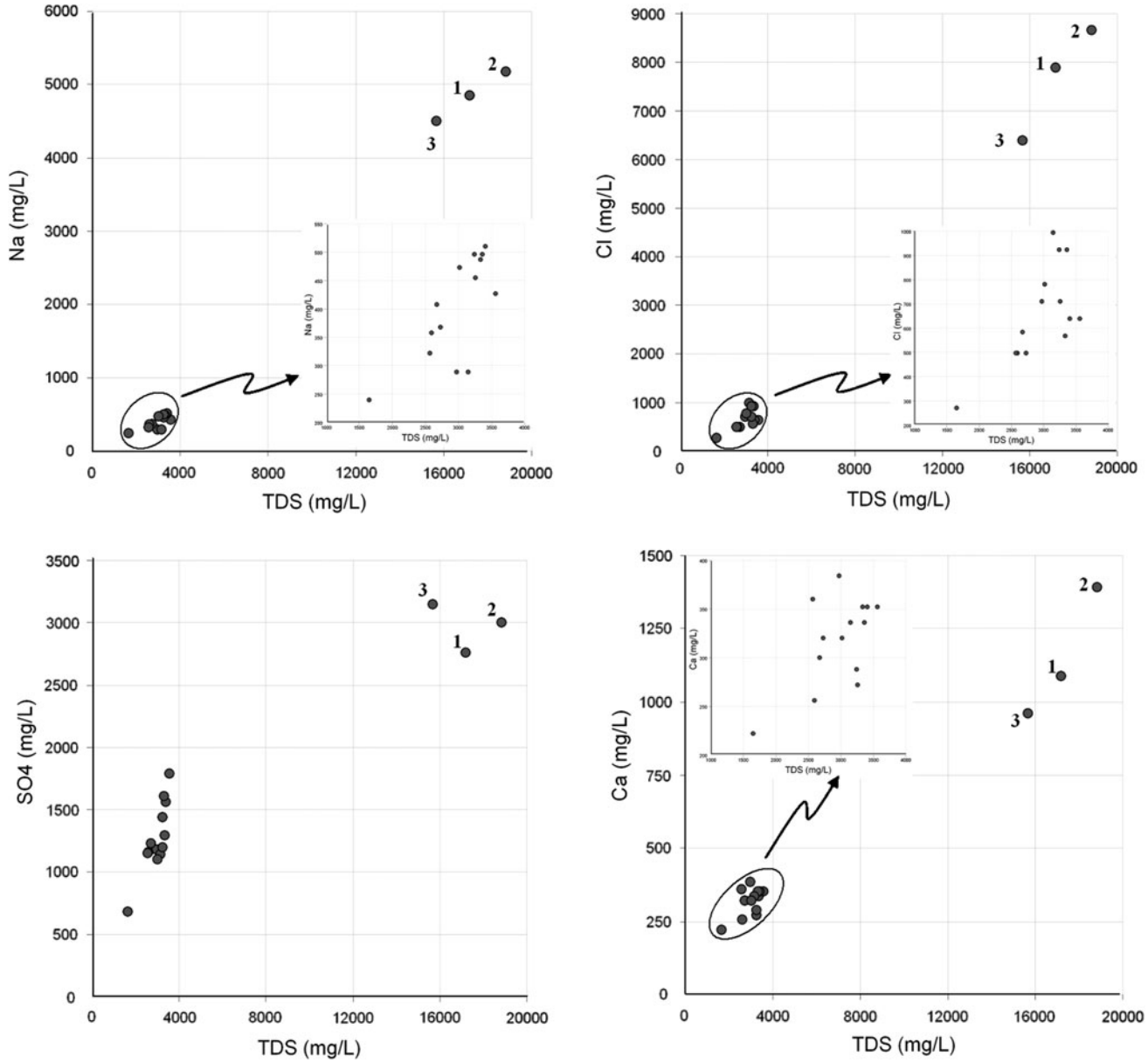

Fig. 6 Major elements versus TDS relationships

Bivariate diagrams of some major elements, directly related to salinity, are used to clarify different mechanisms that control groundwater mineralization. The relationship between major elements and TDS values shows that Na, Cl, Ca and SO_4 are the main contributors to groundwater mineralization (Fig. 6).

– The relationship between Na^+ and Cl^- shows that samples collected from the Menzel Habib-Sbih area cluster along the halite dissolution line (Fig. 7a). The dissolution of this mineral is confirmed by the negative saturation indices (Table 1) indicating an undersaturated state. Also, for those taken from the Matmata area, the molar relationship Na^+/Cl^- shows a rather disperse distribution that can be explained by several phenomena such as the contribution of rainwater to the dilution of waters.

– The relationship between Ca^{2+} and SO_4^{2-} reveals that most cases show predominance of SO_4^{2-} compared to Ca^{2+} (Fig. 7b), probably due to the direct cation exchange reactions that absorb Ca^{2+} on the clay fraction as Na+ is released. Nevertheless, the sample 2, collected in Menzel Habib area have a relative trend to get rich in Ca in relation with the water bearing formations.

Therefore, it seems that the mineralization process of waters in the vicinity of the Hadifa Diapir (in Menzel Habib-Sbih area) has been mainly through the diapiric movement of the evaporitic mass in association with syn-sedimentary extensive tectonic that controls the sector.

On the other hand, it appears that the effect of this Triassic extrusion constitutes, through diverse mixture processes (lateral flow, vertical leakage), a greater threat to coastal groundwater such as in the Skhira basin (Bencheikh et al. 2011).

Isotopic study

Stable isotope composition of water in the study area is quite variable; $\delta^{18}O$ changes from -6.05 to -8.31 ‰ V-SMOW with corresponding δ^2H values changing from −32.5 to −58.6 ‰ V-SMOW. The $\delta^{18}O$ and δ^2H values (Table 1), plotted in Fig. 8 in relation to the global meteoric water line (GMWL: $\delta^2H = 8\delta^{18}O + 10$) (Craig 1961) and the regional meteoric water line of Sfax (SMWL: $\delta^2H = 8\delta^{18}O + 13.5$) (Maliki 2000; Jeanton et al. 2001),

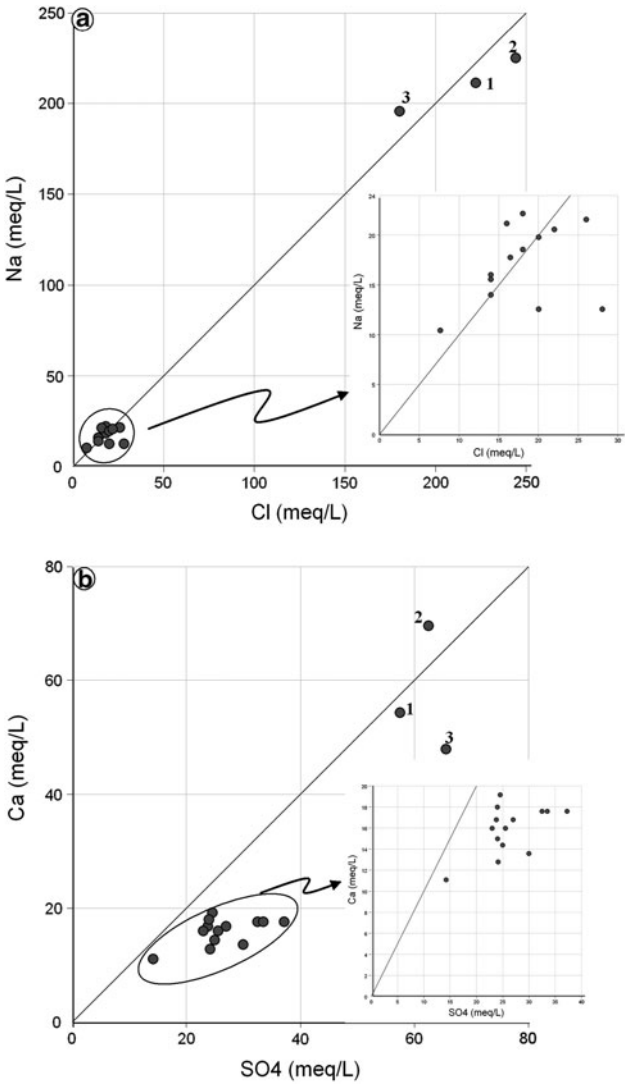

Fig. 7 Relationships between major elements in the analyzed groundwater samples: Na/Cl (**a**), Ca/SO_4 (**b**)

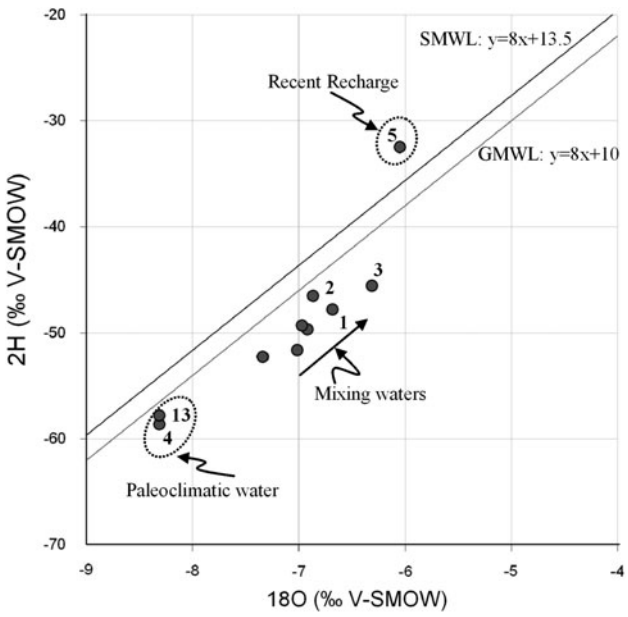

Fig. 8 The δ^2H–$\delta^{18}O$ relationship of the Cenomanian–Turonian groundwater

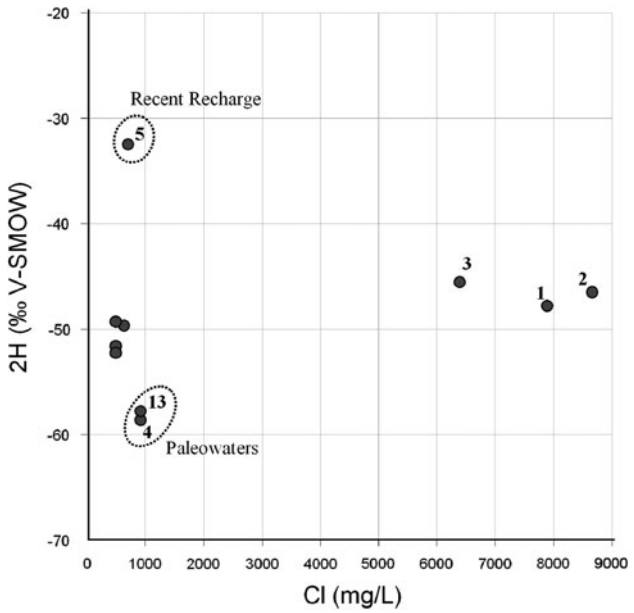

Fig. 9 The δ^2H–Cl relationship of the Cenomanian–Turonian groundwater

show that almost the totality of groundwater samples plot slightly below the GMWL and the RMWL, except for one sample (5) which plotted above the regional meteoric water line. Particularly implanted in the outcropping fissured limestone of the Turonian in the Matmata reliefs (Fig. 1), this sample represents most likely recent infiltration water. This is also confirmed by its highest radiocarbon content (43 pmc) among all measured samples (Abid et al. 2010).

The depleted isotopic signature, distinguished in samples 4 and 13 (El Hamma sector), is typical of old water characteristic of the CI (Continental Intercalaire) aquifer (average stable isotope compositions are, respectively, −8,16 ‰ for $\delta^{18}O$ and −61,2 ‰ for δ^2H (ERESS 1972; Abidi 2001; Edmunds et al. 2003)).

For the other samples, the measured stable isotope composition is quite homogenous. The $\delta^{18}O$ and δ^2H values range, respectively, from −6, 68 to −7, 34 ‰ V-SMOW and from −46, 5 to −52, 23 ‰ V-SMOW. This can be explained by the mixing of new and older waters.

More information is obtained by plotting $\delta\ ^2H$ versus chloride content (Fig. 9). The water samples are divided into different poles with the same distribution observed in Fig. 8: The pole corresponding to the old water, resulting from mixing with Continental Intercalaire groundwater, has average values of −58, 2 ‰ V-SMOW and 923 mg/l, respectively, in $\delta\ ^2H$ and chloride. The second pole, characteristic of recent recharge, shows that the $\delta\ ^2H$ enrichment is due to the effect of rainwater infiltration materialized through the outcropping fissured limestone of the Turonian in the Matmata reliefs.

On the other hand, it is perceptible that the increase of chloride contents, distinguished in the Menzel Habib-Sbih sector, is further evidence that supports the hypothesis of the effect of the outcropping of salt deposits in the Hadifa Diapir to the west.

Conclusion

By its extension, the Cenomanian–Turonian aquifer remains among the most important groundwater systems in southern Tunisia. It represents an important socioeconomic interest in the region. However, the increase in groundwater salinity remains one of the biggest obstacles to its exploitation, particularly in the northern part of this aquifer.

A combined geological, geochemical and isotopic tools have provided a comprehensive understanding of the mineralization processes that control the Cenomanian–Turonian groundwater.

The hydrochemical data permit classifying groundwater into two main water types: Na–Ca–SO_4 and Na–Cl. It appears that the unexpected high salinity of groundwater, distinguished at local scale in the Menzel Habib-Sbih area, is the result of the dissolution of halite. Geological and structural investigations show that the outcropping salt deposits in the Hadifa Diapir to the west are the principal origin of groundwater contamination. In the southern part of the study area, isotopic survey highlights a significant recent recharge materialized through the outcropping fissured limestone of the Turonian in the Matmata reliefs.

Accordingly, this multidisciplinary study underlines that there is no general contamination of groundwater, but rather a local complex situation strictly linked to the geological and structural conditions which control the sector. This source of contamination can be considered as a great threat to bordering aquifers.

In this context, more geochemical and isotopic analyses are required to better solve this problem and quantify the groundwater mineralization rate. Thus, it remains indispensable to find crucial solutions (such as the use of plant species adapted to high salinity and desalination techniques), particularly in the region of Menzel Habib threatened by desertification problem.

Acknowledgments The authors gratefully acknowledge the contributions of the staff members of Gabes and Sfax Water Resources Division/Agriculture Ministry, for their help during fieldwork. We wish to thank the technical staff at the Laboratory of the International Agency of Atomic Energy (IAEA) in Vienna and the Laboratory of Radio-Analyses and Environment of the National Engineering School of Sfax (ENIS) for their help during laboratory analyses.

References

Abbes C, Ben Ouezdou H, Louhaichi M, Mamou A, Lassoued S (1994) Notice explicative de la feuille d'El Hamma de Gabès, n°74 au 1/100.000, 75p, éd. Serv. Géol. Tunisie

Abdallah H, Memmi L, Damotte R, Rat P, Magniez Jannin F (1995) Le Crétacé de la chaine nord des Chotts (Tunisie du centre-sud) : biostratigraphie et comparaison avec les régions voisines. Cretaceous Research 487–538

Abdallah H, Sassi S, Meister C, Souissi R (2000) Stratigraphie séquentielle et paléogéographie à la limite Cénomanien-Turonien dans la région de Gafsa-Chotts (Tunisie centrale), Cretaceous Research 35–106

Abdeljaouad S (1983) Etude sédimentologique et structurale de la partie Est de la chaine Nord des chotts Etude, thèse 3ème cycle, Tunisie. 141 p

Abid K, Zouari K, Dulinski M, Abidi B (2010) Hydrologic and geologic factors controlling groundwater geochemistry in Turonian aquifer (Southern Tunisia). Hydrogeol J 1–13

Abidi B (2001) La nappe du Continental Intercalaire du Sud-Est Tunisien: Analyses de la situation actuelle DGRE, 111

Bencheikh N, Zouari K, Abidi B (2011) Geochemical and isotopic study of paleogroundwater salinization in southeastern Tunisia (Sfax basin). Quaternary International, 1–9

Busson (1967) Mesozoic of Southern Tunisia in Ninth Annual field conference of Petroleum. Exploration Society of Libya

Christian M, Hassen A (1995) Les ammonites du Cénomanien supérieur et du Turonien inférieur de la région de Gafsa-Chotts, Tunisie du Centre Sud. Geobios 29:5

Craig H (1961) Isotopic variations in meteoric water. Science 133:1702–1703

Edmunds W, Guendouz A, Mamou A, Moulla A, Shand P, Zouari K (2003) Groundwater evolution in the Continental Intercalaire aquifer of southern Algeria and Tunisia: trace and isotopic indicators. Appl Geochem 18:805–822

ERESS (1972) Etude des ressources en eau du Sahara Septentrional.UNESCO, Paris

Fontes JC (1971) Un ensemble destiné à la mesure de l'activité du radiocarbone naturel par scintillation liquide. Rev Geog Phys Geol Dyn 67–86

Ihsan S, Abdallah Hassen (2006) The origin of dolomite associated with salt diapirs in central Tunisia: preliminary investigations of field relationships and geochemistry. J Geochem Explor 89(2006):5–9

Jeanton H, Zouari K, Travi Y, Daoud A (2001) Caractérisation isotopique des pluies en Tunisie. Earth and planetary sciences, Essai de typologie dans la région de Sfax, pp 625–631

Louhaichi M, Tlig S (1993) Tectonique synsédimentaire des séries crétacées post-barrémiennes au Nord de la chaîne des chotts (Tunisie méridionale), Géologie Méditerranéenne, 53–74

Maliki A (2000) Etude hydrogéologique, hydrochimique et isotopique de la nappe profonde de Sfax, thèse doct. 254

Ouled Grib Slimane (1994) Nouvelles données géologiques sur l'Atlas méridional de la Tunisie: mise en évidence du Trias dans la chaîne de Gafsa. Notes de service géologique de Tunisie 60:5–10

Zouaghi T, Inoubli M, Bedir M (2007) Contribution of seismic velocity studies to structural and lithostratigraphic reconstructions: salt-intruded corridor ceiling and lower Turonian Beida anhydrite deposits' outline in the central–Southern Atlas of Tunisia. C. R. Geoscience 339(2007):13–23